EXPERIMENTALLY CONSTRAINED (n,γ) REACTION RATES RELEVANT TO r- AND i-PROCESS NUCLEOSYNTHESIS*

M. Guttormsen[a], A.C. Larsen[a], A. Spyrou[b,c,d], S.N. Liddick[b,e]

[a]Department of Physics, University of Oslo, Oslo, Norway
[b]National Superconducting Cyclotron Laboratory, Michigan State University Michigan, USA
[c]Department of Physics and Astronomy, Michigan State University Michigan, USA
[d]Joint Institute for Nuclear Astrophysics, Michigan State University Michigan, USA
[e]Department of Chemistry, Michigan State University, Michigan, USA

(Received January 21, 2020)

The element distribution that we observe in the Universe today tells a fascinating story of nucleosynthesis events that have taken place throughout the 13.7-billion-years-long history starting with the Big Bang. It has been known for a long time that radiative neutron-capture reactions play a major role in synthesizing elements heavier than iron. However, many questions remain when it comes to our understanding of neutron-capture processes in extreme stellar environments. In particular, the intermediate and rapid neutron-capture processes are very challenging to describe, as there exist little or no data on the much-needed neutron-capture rates. In this work, we discuss possibilities to obtain indirect, experimental constrains on these rates by means of the Oslo and the β-Oslo methods.

DOI:10.5506/APhysPolB.51.667

1. Introduction

How and where the elements observed in the Universe were formed remains a significant mystery. The elements are building blocks of all visible matter and essential for life on Earth. The first attempt to determine the distribution of element abundances of our Solar system was made by Goldschmidt in 1937 [1]. It became evident that the isotopic abundance distributions represent fingerprints of the astrophysical processes behind their origin. Over the next twenty years, Burbidge, Burbidge, Fowler and Hoyle

* Presented at the XXXVI Mazurian Lakes Conference on Physics, Piaski, Poland, September 1–7, 2019.

[2] and independently Cameron [3] used new data to lay out the main nucleosynthesis processes. The three processes were identified as:

— the rapid neutron-capture process (r-process),

— the slow neutron-capture process (s-process),

— the proton capture/photodisintegration process (p-process).

The observed element abundances of our Solar system cannot be described by these three processes, only. In 1977, Cowan and Rose [4] proposed that there might be an intermediate neutron-capture process (i-process) with neutron fluxes in between the s- and r-process conditions. The enrichment in Ba (s-process) and Eu (r-process) [5, 6] of some carbon-enhanced metal-poor stars in the Galactic halo and together with the post-AGB star Sakurai's object, all indicate the presence of an i-process [7, 8].

More recently, a neutron-star collision was detected through its gravitational waves by the LIGO and Virgo collaborations [9] in 2017. For the first time, direct observational evidence of the rapid neutron-capture process (r-process) [2, 3, 10] was obtained, proving that neutron-star mergers are producing heavy elements. With this break-through, there is now a pressing need to significantly improve the nuclear-data input required to model the r-process nucleosynthesis. For radiative neutron-capture rates, the presently very large theoretical uncertainties are strongly hampering the predictive power of the nucleosynthesis models [11]. As such, experimental constraints on these neutron-capture rates are highly desired.

The aim of this work is to present techniques for constraining neutron-capture reactions. In particular, we focus on the Oslo and the β-Oslo methods which are promising tools in the study of the astrophysical i- and r-processes. Details on these methods are given in Refs. [12–15] and a recent review of the methods is given in Ref. [16].

2. Indirect estimates of reaction rates

In order to estimate the reaction cross sections, we assume that a compound nucleus is created at high excitation energy with a high number of accessible levels. With these assumptions, we can rely on the Hauser–Feshbach model [17]. Two of the most important ingredients of this model are the nuclear level density ρ and the γ-ray transmission coefficient $\mathcal{T}$. These two quantities can be determined using the Oslo method. Assuming that dipole radiation dominates from high excitation energies, a simple relation between the transmission coefficient and γ-ray strength function is given by $f(E_\gamma) = \frac{1}{2\pi}\mathcal{T}(E_\gamma)/E_\gamma^3$.

Figure 1 shows how a neutron is captured in a nucleus with mass number A and by γ emission, the $A+1$ isotope is formed. The probability that the neutron is captured and stays within the nucleus is proportional to the product of the level density and γ-ray strength function of the $A+1$ system.

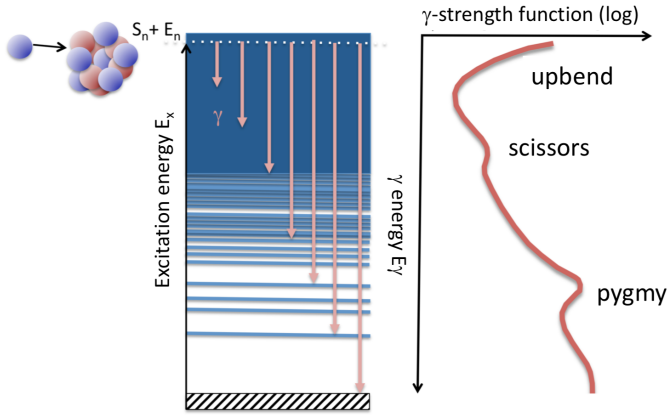

Fig. 1. Illustration of radiative neutron capture [16]. A nucleus captures a neutron and the compound nucleus is excited to an excitation energy given by the neutron separation energy (S_n) and the kinetic energy of the incoming neutron (E_n). The probability for the neutron to stick inside the compound nucleus is proportional to the accessible levels below $S_n + E_n$ and the γ-ray strength function. There are important low-energy structures (marked pygmy, scissors and upbend), which are superimposed on the tail of the giant electric dipole resonance.

3. Experimental set-up and methods

Figure 2 (a) and (b) shows the standard set-up for the Oslo method. As the target nucleus is a stable (or long-lived) isotope, the method is suited for nuclei at or close to the β-stability line. Light-ion reactions accessible at the Oslo Cyclotron Laboratory, such as (p,p'), (p,d) and (^{3}He, α), are used to study the γ-ray energy distribution as a function of initial excitation energy. By choosing neutron-rich targets in combination with *e.g.* the (α,p) reaction, nuclei involved in the i-process may be studied.

A Silicon Ring particle detection system (SiRi) [18], which consists of 64 telescopes, is used for the selection of a certain ejectile type and to determine its kinetic energy. The front ΔE and back E detectors have thicknesses of 130 μm and 1550 μm, respectively. SiRi is usually placed 5 cm from the target in backward angles covering θ = 126–140 degrees relative to the beam direction. Coincidences with the γ rays are performed with the Oslo SCintillator ARray (OSCAR) containing 30 3.5 × 8 inches $LaBr_3$(Ce) detectors.

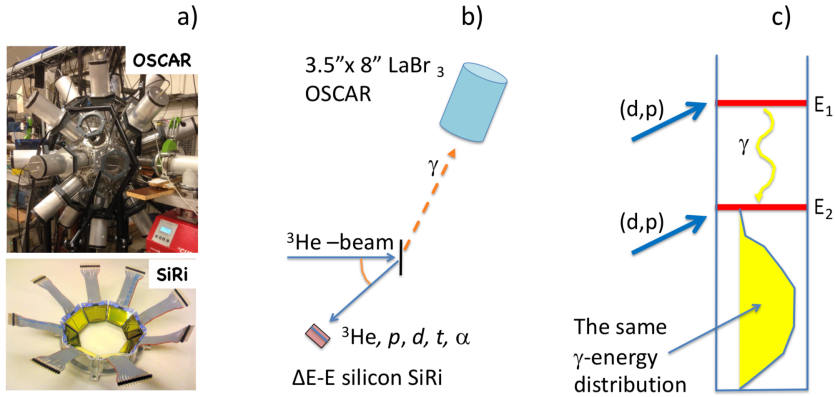

Fig. 2. Typical particle–γ coincidence set-up for a standard Oslo experiment. The 64 silicon particle telescopes of SiRi are placed in the target vacuum chamber at the center of the $LaBr_3$ detector array OSCAR (a). From the charged ejectile, the excitation energy can be determined with the SiRi detectors, and ejectile–γ coincidences are measured (b). The Oslo method rests on the assumption that the γ distribution remains the same if the initial level is populated from γ rays above or directly in the particle reaction (c).

The coincidence data are sorted into a matrix of the γ-ray pulse-heights *versus* E_x with proper subtraction of random coincidences. Then, for all E_x energy bins, the γ-ray pulse-heights spectra are unfolded with the detector response functions. The procedure is iterative and stops when the folding of the unfolded matrix equals the raw matrix within the statistical fluctuations [13]. The raw and unfolded matrices for the $^{148}\mathrm{Nd}(d,p\gamma)^{149}\mathrm{Nd}$ reaction are shown in Fig. 3 (a) and (b), respectively.

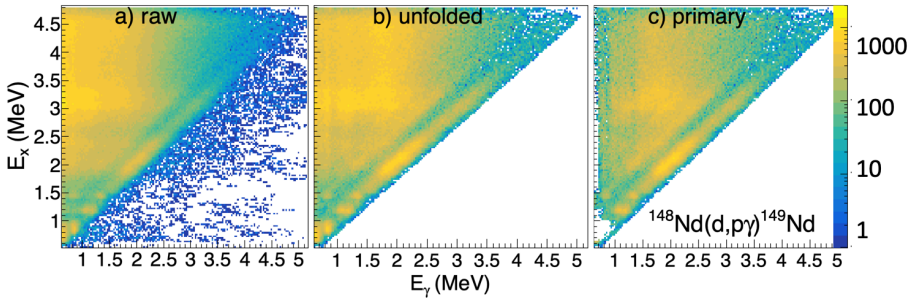

Fig. 3. Initial excitation energy E_x *versus* γ-ray energy E_γ for particle–γ coincidences from the $^{148}\mathrm{Nd}(d,p\gamma)^{149}\mathrm{Nd}$ reaction. The raw γ-ray pulse-heights spectra (a) are first unfolded with the NaI response function (b) and then the primary (or first-generation) γ-ray spectra (c) are extracted as a function of excitation energy. The pixels of excitation energy and γ energy have dispersions of 40 keV/ch.

The unfolded γ matrix, which contains all γ rays of the γ cascades, is the basis for extracting the primary γ matrix containing the energy distribution of the first γ in each cascade. An iterative subtraction technique is applied to remove the higher-generation γ rays by a weighted sum of γ spectra at lower lying excitation energy bins. This weighting function converges rapidly and becomes the very same shape as the primary γ spectra. In this way, the primary γ matrix $P(E_\gamma, E_x)$ can be extracted, as displayed in Fig. 3 (c). More details on the first-generation procedure are found in Ref. [14].

The next step of the Oslo method is the factorization

$$P(E_\gamma, E_x) \propto \rho(E_x - E_\gamma)\mathcal{T}(E_\gamma)\,, \tag{1}$$

which is a strong statement, but rests on reasonable physical assumptions. Firstly, the decay probability is assumed to be proportional to the nuclear level density at the final excitation energy $\rho(E_x - E_\gamma)$ according to Fermi's golden rule [19, 20]. Secondly, the decay is supposed to be proportional to the γ-ray transmission coefficient $\mathcal{T}$, which is set independent of excitation energy according to the Brink hypothesis [21, 22].

The two-dimensional landscape of the primary γ rays as a function of excitation energy (see Fig. 3 (c)) can be now fitted by Eq. (1), giving the functional form of ρ and $\mathcal{T}$. The last step of the Oslo method includes a normalization of these functions to known external data as *e.g.* the complete level scheme at low E_x, the level spacing D_0 at the neutron binding energy S_n and the average γ width $\langle \Gamma_\gamma \rangle$ at S_n. Examples of normalization procedures and the extraction of level densities and γ-ray strength for several nuclei are given in Refs. [23–29].

The extracted ρ and $\mathcal{T}$ functions are used as input to the TALYS nuclear reaction code [30, 31] to calculate radiative capture cross sections. As mentioned, the standard Oslo method is limited to stable or long-lived targets giving only information on nuclei close to the valley of stability. In the following, we describe how the new β-Oslo method can be applied to extract level density and γ-ray strength function for neutron-rich nuclei. As a test case, we will discuss the ^{76}Ge nucleus.

4. The ^{76}Ge case

As described in the previous section, the Oslo-method-type of experiments requires γ spectra from a set of initial excitation energies, usually organized into an (E_γ, E_x) matrix. The idea of the β-Oslo method is to transport a short-lived nucleus into the center of a segmented total absorption spectrometer (TAS). At the moment of the β decay of the short-lived nucleus, individual γ-ray energies (E_γ) and the sum of them ($\sum E_\gamma$) are measured with the TAS. By assuming that the total sum energy represents

the initial excitation energy of the cascades, *i.e.* ($E_x = \sum E_\gamma$), one may construct an (E_γ, E_x) matrix. Ideally, such a TAS should have $\approx$ 100% efficiency and high enough segmentation to cover the typical γ multiplicity expected for β-induced γ cascades.

The β-Oslo method was first applied on ^{76}Ga β-decaying into ^{76}Ge [32]. The population of levels in the ^{76}Ge nucleus is dominantly made by the Gamow–Teller β decay ($\Delta L = 0, 1$, no parity change) from the 2^- ground state of ^{76}Ga. The excited levels will then decay by emitting γ rays through all possible branchings for the initial levels. It should be noted that this would lead to a more constrained range of angular momentum states being populated than in the case of the transfer reactions used in the traditional Oslo method.

The ^{76}Ga experiment was performed at the NSCL (MSU) using a 130 MeV/nucleon ^{76}Ge beam producing ^{76}Ga by fragmentation on a thick beryllium target. The ^{76}Ga secondary beam was first guided through the A1900 fragment separator, and then thermalized in the large-volume gas cell [33] and delivered to the experimental setup, where it was implanted on a silicon surface barrier detector mounted inside SuN, where only the β particles due to the low beam energy (30 keV after the gas cell) were detected. The implantation into the center of SuN is illustrated in the middle part of Fig. 4. SuN was then used to measure the subsequent γ-ray cascades in the daughter nucleus ^{76}Ge, as shown in the right part of Fig. 4. The measured level density and γ-ray strength function of ^{76}Ge using the SuN data as input in TALYS reduced the previous uncertainties in the reaction rates from a factor of $\approx$ 10 down to a factor of $\approx$ 2, see Ref. [32] for more details.

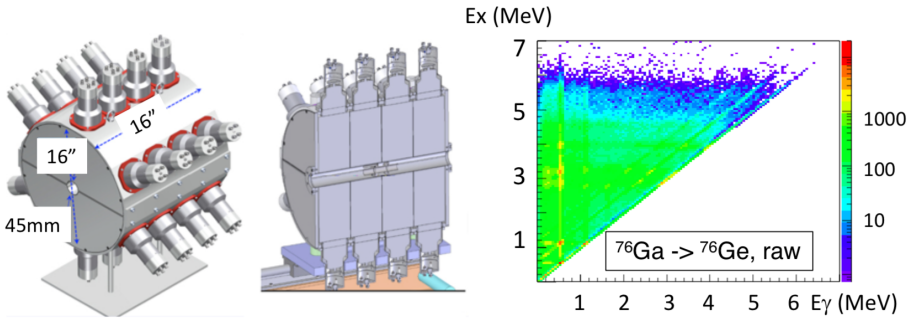

Fig. 4. The Summing NaI detector (SuN) is a total absorption spectrometer constructed from a cylinder of NaI(Tl) 16 inches in diameter and 16 inches in length (left panel) [34]. A small silicon detector (SSB) was mounted in the center of SuN to stop the incoming ion and detect the subsequent β-decay electron (middle panel). The beam of ^{76}Ga is implanted in the center of SuN and an (E_x, E_γ) matrix of ^{76}Ge was measured (right panel)

In the β-Oslo method, E_x is deduced from the sum of γ-rays within a β-decay event. This fact leaves us with a challenge in analysing the data. First of all, the deduced excitation energy will be too low if some of the γ-ray energies are not fully detected due to *e.g.* Compton scattering. Furthermore, the electron from the β decay may interact with the NaI crystals, inducing an additional background. Finally, the technique rests on the assumption that single γ rays are measured by individual scintillator segments, which may be violated for high γ-multiplicity events giving pile-up in the same segment. Therefore, in order to correct for these short-comings, we unfold the E_x spectrum in addition to the usual unfolding of the E_γ spectrum.

A new approach [35] is now implemented in the Oslo-method software [36]. In order to unfold the excitation energies, we have made Geant4 simulations for various E_x, M_γ, and Q_β values, in total 340 spectra. For a given reaction, we interpolate between these spectra to obtain a response matrix as shown in Fig. 5 (a). The matrix is calculated for ^{76}Ge with the assumption of a certain multiplicity function $M_\gamma(E_x)$. Panel (b) demonstrates that a high-energy tail is present in the response function for high Q-values, here $Q_\beta = 12$ MeV.

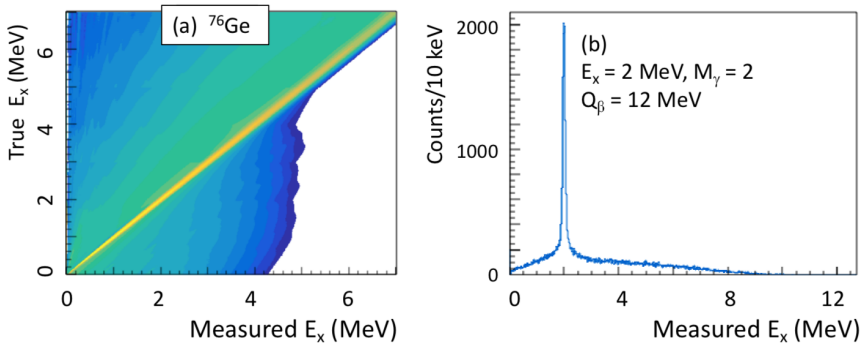

Fig. 5. The excitation energy response matrix for $Q_\beta = 6.916$ MeV is shown in (a). A specific response function for $E_x = 2$ MeV, $M_\gamma = 2$, and $Q_\beta = 12$ MeV (b) showing energy tails on both sides of the true excitation energy.

The impact of introducing unfolding along the E_x axis is shown in Fig. 6 for the ^{70}Ni case [37]. We find a strong improvement when extracting the level density since the incomplete summing is rather well-removed from the matrix. However, one should keep in mind that the subsequent unfolding along each of the axis is a simplification of the problem. The measured E_γ and E_x values turns out to have a complex interplay that is not described by the new unfolding technique. We are, therefore, currently working on a machine-learning approach for improving the unfolding of the raw (E_γ, E_x) matrices of the β-Oslo method.

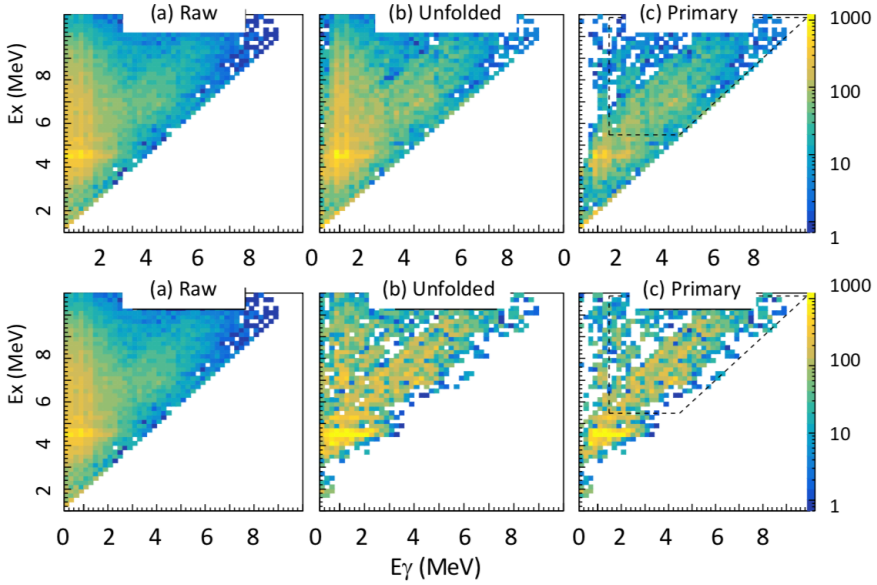

Fig. 6. Upper panels show the raw (a), unfolded (b) and the first-generation (c) γ matrices obtained by unfolding the γ-energy axis E_γ only. By first unfolding the excitation axis E_x and then the γ-energy axis E_γ, we obtain new and more realistic unfolded and first-generation matrices, see lower panels.

5. Summary and conclusions

The standard Oslo method has proven to be a successful tool in extracting level density and γ-strength function for nuclei in the region of the β-stability line. For nuclei populated via β^- decay, the β-Oslo method using total absorption spectrometers can be used to extract the same quantities. By assuming the population of a compound nucleus, the Hauser–Feshbach model with the input from experiments can be used to constrain the reaction rates relevant to the r- and i-process nucleosynthesis.

A.C.L. gratefully acknowledges funding through ERC-STG-2014 under grant agreement No. 637686 and support from the ChETEC COST Action (CA16117) supported by COST (European Cooperation in Science and Technology), and grant No. OISE-1927130 (IReNA). This work was supported by the National Science Foundation under grants No. PHY 1102511 (NSCL) and No. PHY 1430152 (Joint Institute for Nuclear Astrophysics), and PHY 1350234 (CAREER). The authors would like to thank F.L. Bello Garrote, A. Görgen, V.W. Ingeberg, J.E. Midtbø, V. Modamio, T. Renstrøm, E. Sahin, S. Siem, O. Sorlin, G.M. Tveten, M. Wiedeking and F. Zeiser for stimulating discussions.

REFERENCES

[1] V.M. Goldschmidt, Skrifter Norske Vitenskapsakad., Oslo, I. Mat.-Naturv. Kl., No. 4 (1937).

[2] E.M. Burbidge, G.R. Burbidge, W.A. Fowler, F. Hoyle, *Rev. Mod. Phys.* **29**, 547 (1957).

[3] A.G.W. Cameron, *Publ. Astron. Soc. Pac.* **69**, 201 (1957).

[4] J.J. Cowan, W.K. Rose, *Astrophys. J.* **212**, 149 (1977).

[5] C. Abate *et al.*, *Astron. Astrophys.* **587**, A50 (2016).

[6] M. Hampel *et al.*, *Astrophys. J.* **831**, 171 (2016).

[7] F. Herwig *et al.*, *Astrophys. J.* **727**, 89 (2011).

[8] P. Denissenkov *et al.*, *J. Phys. G: Nucl. Part. Phys.* **45**, 055203 (2018).

[9] B.P. Abbott *et al.* [LIGO Scientific Collaboration and Virgo Collaboration], *Phys. Rev. Lett.* **119**, 161101 (2017).

[10] D. Watson *et al.*, *Nature* **574**, 497 (2019) and references therein.

[11] M. Mumpower, R. Surman, G. McLaughlin, A. Aprahamian, *Prog. Part. Nucl. Phys.* **86**, 86 (2016).

[12] A. Schiller *et al.*, *Nucl. Instrum. Methods Phys. Res. A* **447**, 498 (2000).

[13] M. Guttormsen *et al.*, *Nucl. Instrum. Methods Phys. Res. A* **374**, 371 (1996).

[14] M. Guttormsen, T. Ramsøy, J. Rekstad, *Nucl. Instrum. Methods Phys. Res. A* **255**, 518 (1987).

[15] A.C. Larsen *et al.*, *Phys. Rev. C* **83**, 034315 (2011).

[16] A.C. Larsen, A. Spyrou, S.N. Liddick, M. Guttormsen, *Prog. Part. Nucl. Phys.* **107**, 69 (2019).

[17] W. Hauser, H. Feshbach, *Phys. Rev.* **87**, 366 (1952).

[18] M. Guttormsen, A. Bürger, T.E. Hansen, N. Lietaer, *Nucl. Instrum. Methods Phys. Res. A* **648**, 168 (2011).

[19] P.A.M. Dirac, *Proc. R. Soc. Lond. A* **114**, 243 (1927).

[20] E. Fermi, *Nuclear Physics*, University of Chicago Press, 1950.

[21] D.M. Brink, Ph.D. Thesis, Oxford University, 1955.

[22] M. Guttormsen *et al.*, *Phys. Rev. Lett.* **116**, 012502 (2016).

[23] H. Utsunomiya *et al.*, *Phys. Rev. C* **88**, 015805 (2013).

[24] T.G. Tornyi *et al.*, *Phys. Rev. C* **89**, 044323 (2014).

[25] T.A. Laplace *et al.*, *Phys. Rev. C* **93**, 014323 (2016).

[26] A.C. Larsen *et al.*, *Phys. Rev. C* **93**, 045810 (2016).

[27] G.M. Tveten *et al.*, *Phys. Rev. C* **94**, 025804 (2016).

[28] L. Crespo Campo *et al.*, *Phys. Rev. C* **94**, 044321 (2016).

[29] T. Renstrøm *et al.*, *Phys. Rev. C* **93**, 064302 (2016).

[30] A.J. Koning, S. Hilaire, M.C. Duijvestijn, TALYS-1.6, in: Proceedings of the International Conference on Nuclear Data for Science and Technology, April 22–27, 2007, Nice, France, (Eds.) O. Bersillon, F. Gunsing, E. Bauge, R. Jacqmin, S. Leray, EDP Sciences, 211, 2008.

[31] A.J. Koning, D. Rochman, *Nucl. Data Sheets* **113**, 2841 (2012).

[32] A. Spyrou *et al.*, *Phys. Rev. Lett.* **113**, 232502 (2014).

[33] K. Cooper *et al.*, *Nucl. Instrum. Methods Phys. Res. A* **763**, 543 (2014).

[34] A. Simon *et al.*, *Nucl. Instrum. Methods Phys. Res. A* **703**, 16 (2013).

[35] M. Guttormsen *et al.*, work in progress.

[36] M. Guttormsen *et al.*, 2019, https://zenodo.org/badge/DOI/10.5281/zenodo.2318646.svg

[37] A.C. Larsen *et al.*, *Phys. Rev. C* **97**, 054329 (2018).